A Hybrid Index for Characterizing Drought Based on a Nonparametric Kernel Estimator

SHENGZHI HUANG AND QIANG HUANG

State Key Laboratory Base of Eco-Hydraulic Engineering in Arid Area, Xi'an University of Technology, Xi'an, China

GUOYONG LENG

Joint Global Change Research Institute, Pacific Northwest National Laboratory, College Park, Maryland

JIANXIA CHANG

State Key Laboratory Base of Eco-Hydraulic Engineering in Arid Area, Xi'an University of Technology, Xi'an, China

ABSTRACT

This study develops a nonparametric multivariate drought index, namely, the nonparametric multivariate standardized drought index (NMSDI), by considering the variations of both precipitation and streamflow. Building upon previous efforts in constructing nonparametric multivariate drought index, the nonparametric kernel estimator is used to derive the joint distribution of precipitation and streamflow, thus providing additional insights into drought-index development. The proposed NMSDI is applied in the Wei River basin (WRB), on the basis of which the drought-evolution characteristics are investigated. Three main results were found: 1) In general, NMSDI captures drought onset in a way that is similar to that of the standardized precipitation index and captures drought termination and persistence in a way that is similar to that of the standardized streamflow index. The drought events identified by NMSDI match well with historical drought records in the WRB. Performance is also consistent with that of an existing multivariate standardized drought index at various time scales, confirming the validity of the newly constructed NMSDI in drought detections. 2) An increasing risk of drought has been detected for past decades and will persist to a certain extent in the future in most areas of the WRB. 3) The identified changepoints of annual NMSDI are mainly concentrated in the early 1970s and mid-1990s, coincident with extensive water use and soil conservation practices. In summary, this study highlights a nonparametric multivariable drought index that can efficiently and comprehensively be used for drought detections and predictions.

1. Introduction

Drought, caused by water deficit over extended periods, has huge adverse impacts on agriculture, society, the economy, and ecosystems (Wilhite 2000; Mishra and Singh 2010; Dai 2011; Sheffield et al. 2012). According to an assessment by the Ministry of Water Resources of China, annual grain loss induced by drought in China is nearly 39.2×10^9 kg, and the average economic loss is about 1.47% of the country's gross domestic product. With global warming, China is projected to experience more frequent, pronounced, and severe droughts, with long-term droughts increasing more than short-term droughts (Leng et al. 2015, 2016). Drought monitoring and prediction are therefore of great importance for taking prompt and effective measures to reduce the influence of droughts (WMO 2006; AghaKouchak and Nakhjiri 2012; Sheffield et al. 2014; Huang et al. 2014a,b).

Although there is a strong desire to develop an algorithm that can be used to accurately describe and assess

Corresponding author address: Guoyong Leng, Joint Global Change Research Institute, Pacific Northwest National Laboratory, 5825 University Research Court, Suite 3500, College Park, MD 20740.
E-mail: guoyong.leng@pnnl.gov

droughts, it is unfortunately not easy to achieve by means of either statistical or physical analyses. The primary obstacle is lack of a universally accepted definition of droughts (Wells et al. 2004; Vicente-Serrano et al. 2010; Mishra and Singh 2010, 2011; Winslow et al. 2011; Sherwood and Fu 2014; Spinoni et al. 2014; van der Schrier et al. 2013; Hao and Singh 2015). A drought indicator is extremely critical and fundamental for drought monitoring and prediction because of its ability to simplify complex interplay among many hydroclimatic parameters. Drought indices allow the quantitative evaluation of droughts in terms of frequency, duration, severity, and spatial extent (Wilhite 2000).

Various drought indices have been developed and adopted for drought characterization and monitoring. The Palmer drought severity index is used and applied in drought assessment and monitoring studies (Palmer 1968; Dai 2011). The standardized precipitation index (SPI) proposed by McKee et al. (1993) is used for meteorological drought characterization and has been demonstrated to be an effective tool for identifying the early onset of drought (Shukla et al. 2011; Hao and AghaKouchak 2014). The standardization concept of the SPI has been extended to other variables to develop drought indices such as the standardized runoff index (Shukla and Wood 2008), the standardized streamflow index (SSFI; Telesca et al. 2012), and the standardized soil moisture index (SSI; Hao and AghaKouchak 2013) for hydrological and/or agricultural drought characterization.

Drought indicators that are based on different variables differ in performance in identifying drought onset and termination. A meteorological drought (shortage in precipitation) may develop and end quickly, whereas the onset and persistence of a hydrologic drought (deficit in streamflow) respond to a meteorological drought with some delays (Pandey and Ramasastri 2001; Heim 2002). A drought index that is based on precipitation shortage is appropriate for capturing drought onset, whereas a drought index that is based on streamflow shortage is efficient for detecting drought persistence. The discrepancies in the physical bases of drought-related variables make it difficult to construct an efficient and comprehensive drought index that is based on one single variable (e.g., precipitation or streamflow). Wilhite (2005) pointed out that utilization of a single index is one of the major obstacles for accurate drought characterization and prediction. It is well recognized that no single index can characterize all aspects of meteorological, hydrological, and agricultural droughts and that a multivariable approach should be adopted to cope with this issue (Quiring et al. 2007; Hao and AghaKouchak 2013).

Several efforts have recently been made to develop a variety of integrated drought indicators that combine multiple drought-related variables (e.g., precipitation, soil moisture, and streamflow); these include the standardized precipitation evapotranspiration index (Vicente-Serrano et al. 2010), the aggregate drought index (Keyantash and Dracup 2004), the combined drought indicator (Sepulcre-Canto et al. 2012), the joint deficit index (Kao and Govindaraju 2010), and the multivariate standardized drought index (MSDI; Hao and AghaKouchak 2014). The MSDI, which is based on copula functions, has been demonstrated in practice to be an effective tool for drought prediction and monitoring (AghaKouchak 2015; Hao and Singh 2015). It is capable of denoting droughts at a specific time scale, which is similar to SPI but is extended to a bivariate version that combines information on precipitation and soil moisture. Copulas, which are in essence a parametric approach, strongly rely on the assumption that data samples follow a particular probability density function (PDF; Huang et al. 2014a). Because the complex interrelationships among atmosphere, vegetation, surface water, soil, and groundwater have large impacts on drought processes, any of the given distributions may fail to accurately reflect drought conditions (Sadri and Burn 2012). In fact, no worldwide parametric distribution exists for hydrologic and meteorological variables (Silverman 1986; Moon and Lall 1994; Smakhtin 2001; Farahmand and AghaKouchak 2015). Application of a parametric distribution tends to cause a big deviation of tails such as the low or high quantiles (Sharma 2000).

To our knowledge, only Hao and AghaKouchak (2014) have introduced a nonparametric multivariate drought index, which in their work is based on an empirical joint probability in the bivariate case using the Gringorten plotting-position formula. Being based on the weighted moving means of sample data from a small neighborhood of the estimated point, nonparametric function estimation has the advantage of reproducing the attributes denoted by the sample (Lall 1995; Sharma 2000). In this study, we build upon the efforts of Hao and AghaKouchak (2014) by proposing an additional nonparametric multivariate drought index using a kernel estimator. The majority of nonparametric density-estimation methods can be expressed through a kernel-density estimator that entails a weighted moving mean of an empirical frequency distribution of the sample data (Scott 1992; Sharma 2000). Our study complements existing research and can provide additional insights for drought-index development. The newly proposed drought index was applied in the Wei River basin (WRB), on the basis of which the drought evolution characteristics—including its trends, persistence, and period—are then investigated.
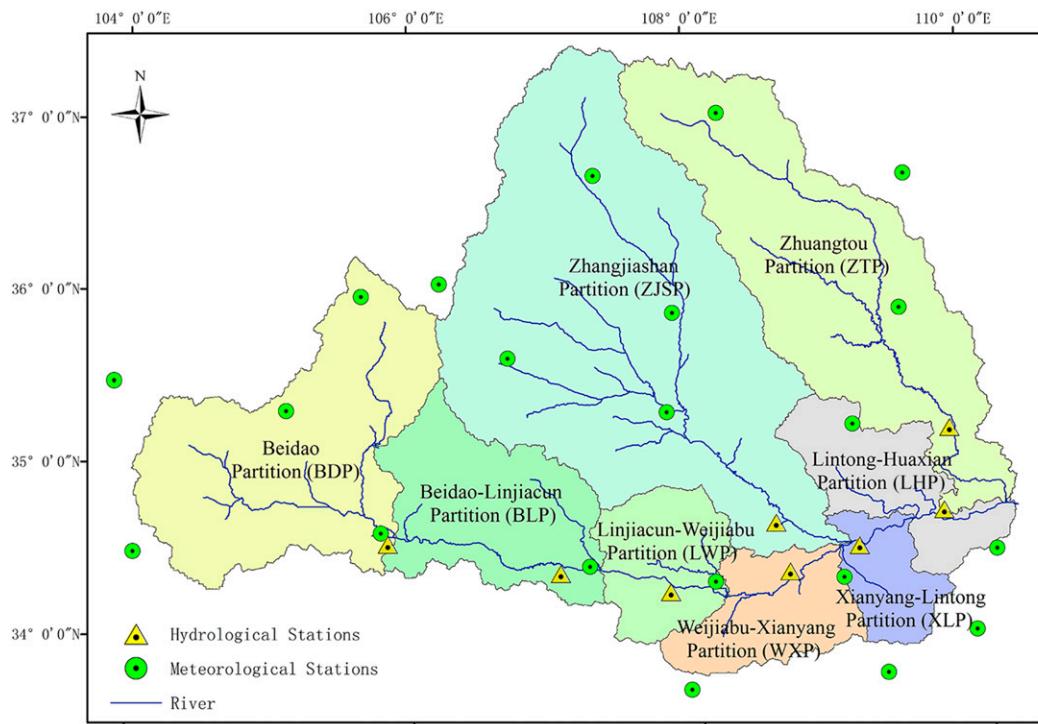
FIG. 1. The study region and locations of hydrometeorological stations.

2. Study area and data

The WRB lies between 103.5° and 110.5°E and between 33.5° and 37.5°N (Fig. 1), with a total land area up to 1.35×10^5 km^2. The altitude increases from the lowest Guanzhong Plain south of the basin to the highest northwest mountainous areas. The regional mean annual precipitation of the basin is approximately 559 mm, with a decreasing trend for the past decades (Zhang et al. 2008).

In this study, observed precipitation records from 21 meteorological stations in the WRB are obtained from the National Climate Center of the China Meteorological Administration (Fig. 1). The records covering the period from 1960 to 2010 at the daily time step have been used well in characterizing the spatial–temporal hydroclimatic changes in the WRB (e.g., Chang et al. 2014). Daily observed streamflow series for Beidao (BD), Linjiacun (LC), Weijiapu (WP), Zhangjiashan (ZJS), Xianyang (XY), Lintong (LT), Huaxian (HX), and Zhuangtou (ZT) hydrological stations in the main stream and major tributaries of the WRB were obtained from the Yellow River Conservancy Commission. To be specific, the BD, LC, WP, XY, LT, and HX stations are located in the main stream and the ZJS and ZT stations respectively lie in the Jinghe River and Beiluohe River first-grade tributaries (Fig. 1). Figure 1 also shows the boundary of eight subareas for our detailed investigation in this study.

3. Methods

a. Nonparametric multivariate standardized drought index (NMSDI)

1) UNIVARIATE KERNEL ESTIMATOR

Nonparametric function estimates, which are based on weighted moving-mean values, have the advantage that they can effectively capture the attributes of the sample (Lall 1995; Kim et al. 2003) and have been used well in hydrology for frequency analysis (Lall 1995). A kernel-density estimator is the key in most nonparametric density-estimate approaches in calculating the weighted moving mean of the empirical frequency distribution of the given sample (Scott 1992; Kim et al. 2003). By intercomparing with the parametric Gumbel, lognormal, and Pearson III distributions, Kim et al. (2003) demonstrated that the nonparametric kernel estimator has a better performance in fitting the PDF of input time series.

Given n observations $x_1, \ldots, x_n$, the univariate kernel-probability-density estimator can be derived as

$$\hat{f}_X(x) = \frac{1}{nh} \sum_{i=1}^{n} K\left(\frac{x - x_i}{h}\right), \qquad (1)$$

where K is a kernel function and h is the bandwidth controlling the variance of that kernel function. Previous

TABLE 1. Examples of univariate kernel functions.

Kernel	$K(t)$
Epanechnikov	$K(t) = 0.75(1 - t^2)$ for $|t| \leq 1$; $K(t) = 0$ otherwise
Triangular	$K(t) = 1 - |t|$ for $|t| \leq 1$; $K(t) = 0$ otherwise
Gaussian (normal)	$K(t) = (2\pi)^{-1/2} e^{-(t \times t)/2}$
Rectangular	$K(t) = 0.5$ for $|t| \leq 1$; $K(t) = 0$ otherwise

TABLE 2. Classification of the NMSDI.

Category	Index value
Extreme drought	NMSDI ≤ -2.0
Severe drought	$-2.0 <$ NMSDI ≤ -1.5
Moderate drought	$-1.5 <$ NMSDI ≤ -1.0
Near normal	$-1.0 <$ NMSDI ≤ 1.0
Moderately wet	$1.0 <$ NMSDI ≤ 1.5
Very wet	$1.5 <$ NMSDI ≤ 2.0
Extremely wet	NMSDI ≥ 2.0

studies applying the kernel functions in the water-resources and hydrology research fields are summarized in Table 1 (Silverman 1986; Lall et al. 1996). In this study, we use the Gaussian kernel function following the method of Kim et al. (2003). With a decrease in h, the assessed function tends to exhibit a variance that resembles the individual observations, and vice versa. In a given data space, a larger h would lead to a smoother function. With K as the Gaussian density, the estimation of h is expressed as

$$h_d = \left[\frac{4}{n(p+2)}\right]^{1/(p+4)} \sigma_d, \tag{2}$$

where h_d is the optimal bandwidth, p is the number of dimensions (with $p = 1$ and 2 indicating the univariate and bivariate kernel estimators, respectively), and σ_d is the standard deviation of the distribution in dimension d.

2) BIVARIATE KERNEL ESTIMATOR

Bivariate kernel-density estimators are constructed with a similar approach to that of the univariate estimators but on the basis of a set of bandwidths (h_x, h_y). The joint PDF for two variables of interest (precipitation and streamflow in this study) is computed as

$$\hat{f}_{XY}(x, y) = \frac{1}{nh_x h_y} \sum_{i=1}^{n} \left[K\left(\frac{x - x_i}{h_x}\right) K\left(\frac{y - y_i}{h_y}\right) \right], \tag{3}$$

where n is the total number of observations (x_i, y_i), K is the Gaussian kernel function, and h_x and h_y are the bandwidths for variables x and y, respectively. The determination of h is as in Kim et al. (2003); h depends on the sample data, and only one optimal value is derived.

3) CALCULATION OF NMSDI

Through constructing the joint PDF of precipitation and streamflow using the bivariate kernel-density estimators, their joint cumulative distribution function (CDF) is expressed as

$$P(X \leq x, Y \leq y) = p, \tag{4}$$

where p is the joint CDF of precipitation (variable x) and streamflow (variable y). The NMSDI is then calculated as

$$\text{NMSDI} = \phi^{-1}(p), \tag{5}$$

where ϕ^{-1} is the inverse of the standard normal distribution function. The derivation of NMSDI is similar to the SPI (McKee et al. 1993; Huang et al. 2014a) but is based on a multivariate distribution function. Classification of the developed NMSDI is shown in Table 2.

The trends of NMSDI are detected using the modified Mann–Kendall (MMK) trend-test method (Mann 1945; Kendall 1955; Hamed and Rao 1998). Unlike the original Mann–Kendall trend-test method, the MMK trend-test method can overcome issues arising from the persistence of the hydrometeorological series (Hamed and Rao 1998). Wavelet analysis (Torrence and Compo 1998) is used to reveal the periodic characteristics of droughts as based on the annual NMSDI. The technique can give a quantitative measure of changes in variance on interdecadal time scales. The MMK and wavelet-analysis techniques have been used well in our previous studies (Huang et al. 2014b).

b. The rescaled range (R/S) analysis

The R/S analysis (Hurst 1956) has been widely used in the fields of morphology, cell reproduction, hydrology, and earthquake activity in forecasting their long-memory processes (Hosking 1984; Wang et al. 2013). The basic idea of the R/S analysis is to change the time scale of a given series on the basis of an examination of its statistical characteristics (Oliver and Ballester 1996).

For a time series with n observations $X = x_1, x_2, \ldots, x_n$, the average series is calculated as

$$y(\tau) = \frac{1}{\tau} \sum_{t=1}^{\tau} x(t) \quad \tau = 1, 2, \ldots. \tag{6}$$

The deviation is calculated as

$$F(t, \tau) = \sum_{t=1}^{\tau} x(t) \quad 1 \leq t \leq \tau. \tag{7}$$

The range is calculated as

$$R(\tau) = \max_{1 \le t \le \tau} F(t, \tau) - \min_{1 \le t \le \tau} F(t, \tau). \qquad (8)$$

Its standard deviation is calculated as

$$S(\tau) = \left| \frac{1}{\tau} \sum_{t=1}^{\tau} [x(t) - y(\tau)]^2 \right|^{1/2}. \qquad (9)$$

The rescaled range, as based on its standard deviation and range, is calculated as

$$R(\tau)/S(\tau) = (C\tau)^H, \qquad (10)$$

where C is a constant and H is the calculated Hurst index.

A value of the Hurst index that is greater than 0.5 indicates that the characteristics of future change are expected to be similar to those in the past, and a larger H value in the range of 0.5–1.0 indicates higher probabilities of this tendency. A value of the Hurst index that is equal to 0.5 indicates that the series is totally independent. A value of the Hurst index that is less than 0.5 denotes that the change trend in the future would be opposite to that of the past, and a smaller H in the range of 0–0.5 indicates higher probabilities of this tendency (Oliver and Ballester 1996).

c. The heuristic segmentation method

Existing statistical-test approaches such as the sliding F test and sliding t test are frequently adopted for detecting the changepoints. The assumption of stationarity has to be made, however, which is not true in hydrologic time series with nonlinear features because of the high variability in the hydrologic process (Feng et al. 2005). The heuristic segmentation method proposed by Bernaola-Galván et al. (2001) is based on the sliding t test but is modified to partition a nonstationary series into several stationary series, thus overcoming the drawbacks of the above methods.

To divide a nonstationary time series into several stationary segments, a sliding pointer is designed that moves step by step along the time series from its left side to its right side (Bernaola-Galván et al. 2001). The average values of the subsets to the left of the pointer (designated as μ_1) and to the right (μ_2) are then calculated. The difference between the averages of the two series μ_1 and μ_2 is estimated using the Student's t-test statistic as follows:

$$t = \left| \frac{\mu_1 - \mu_2}{S_D} \right|, \quad \text{where} \qquad (11)$$

$$S_D = \left[\frac{(N_1 - 1)s_1^2 + (N_2 - 1)s_2^2}{N_1 + N_2 - 2} \right]^{1/2} \left(\frac{1}{N_1} + \frac{1}{N_2} \right)^{1/2} \qquad (12)$$

is the pooled variance, N_1 and N_2 are the number of points of the two series, and s_1 and s_2 are the standard deviations of the two series. A larger t indicates more statistically different mean values between the two time series. Hence, the largest t value is taken as the cut point, on the basis of which the statistical significance $P(t_{\max})$ is calculated. Note that $P(t_{\max})$ is not the standard Student's t test because the series are not independent and cannot be derived in a closed analytical form; therefore, $P(t_{\max})$ is approximately calculated as

$$P(t_{\max}) \approx \{ 1 - I_{[\upsilon/(\upsilon + t_{\max}^2)]}(\delta\upsilon, \delta) \}^{\eta}, \qquad (13)$$

where $\eta = 4.19 \ln N - 11.54$ and $\delta = 0.4$ are obtained from the Monte Carlo simulations, N is the length of the time series, $\upsilon = N - 2$, and $I_x(a, b)$ is the incomplete beta function (Bernaola-Galván et al. 2001). No split is made to the time series if the difference of the mean values is not statistically significant [i.e., $P(t_{\max})$ is smaller than a threshold of 0.95]. Conversely, the time series is cut into two segments, and the iteration of the above procedures continues on each new segment until the significant value is smaller than the threshold or the length of the new segments is smaller than the predefined minimum segment length ℓ_0.

4. Results and discussion

a. The performance of the NMSDI

Figure 2a shows the time series of 1-month NMSDI, the MSDI developed by Hao and AghaKouchak (2013), SPI, and SSFI covering 1960–2011 for the whole Wei River basin. It is found that the change pattern of 1-month NMSDI is generally consistent with that of 1-month SPI or SSFI as well as MSDI. The correlation coefficients of MSDI with SPI and SSFI are 0.80 and 0.79, respectively. The performance of NMSDI is comparable to MSDI, and the correlation coefficients with SPI and SSFI are up to 0.83 and 0.81, respectively, indicating the reliability of the newly constructed NMSDI. For better visual comparisons, the 1-month NMSDI, MSDI, SPI, and SSFI values covering 2002–11 are shown in Fig. 2b. Some discrepancies are found among the four drought indices. In general, because a persistent deficit of precipitation is commonly the beginning of drought, SPI is sensitive to capturing the drought onset, whereas SSFI is effective in identifying drought persistence, mainly because of the complex runoff process (Hao and AghaKouchak 2013). As shown by the black rectangles in Fig. 2b, the timing of NMSDI and SPI values that are smaller than −1 (which is identified as drought onset) is earlier than that of SSFI, indicating that NMSDI captures the onset of drought as early as SPI does. In addition,
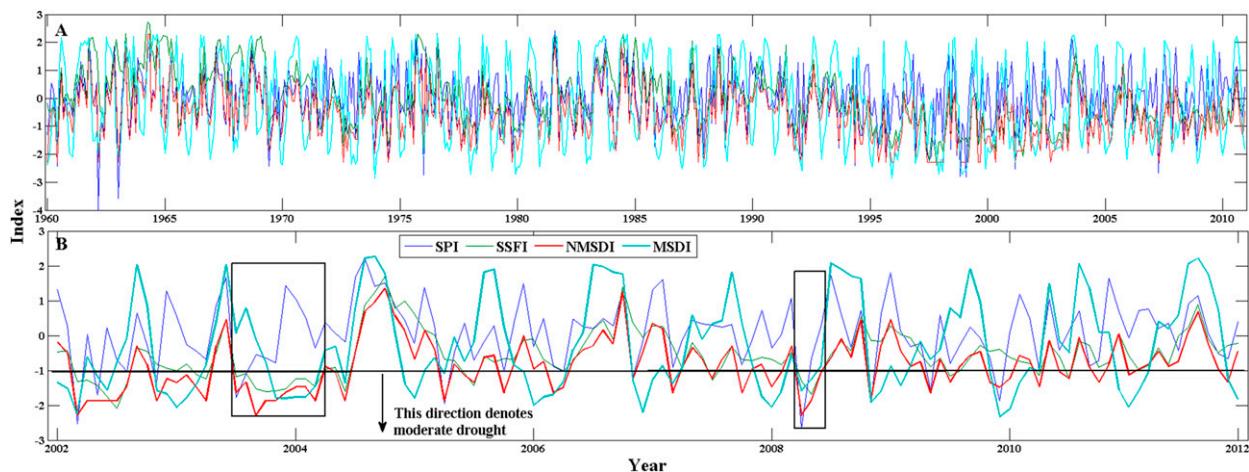
FIG. 2. Comparison of 1-month NMSDI, MSDI, SPI, and SSFI series covering (a) 1960–2011 and (b) 2002–11 in the whole WRB; the solid black horizontal line is the threshold of moderate drought in the drought indices.

the timing of NMSDI and SSFI with values of larger than −1 is later than that of SPI, indicating that NMSDI captures the termination of drought in a way that is similar to SSFI. The performances of NMSDI are also consistent with MSDI at various time scales. That is, NMSDI captures well drought onset similar to SPI and drought termination and persistence similar to SSFI. Note that NMSDI is more sensitive in capturing drought onset and termination than MSDI is at the 1-month time scale, demonstrating the added value of the nonparametric approach with kernel estimator in drought characteristics. By examining the temporal variability of NMSDI, MSDI, SPI, and SSFI at the subbasin level, similar findings are obtained (the figures are not shown for brevity). Because NMSDI is coupled with information on both precipitation and streamflow, it is sensitive and effective in capturing the onset, persistence, and termination of droughts, and similar features are also exhibited at the 3- and 6-month scales (Fig. 3). Statistics show that the drought frequency identified by SPI is the highest whereas that identified by SSFI is the lowest (Table 3). This is because meteorological droughts characterized by SPI develop quickly and end abruptly, whereas hydrological droughts characterized by SSFI respond to meteorological droughts with some lag time and show a strong persistence (Heim 2002). Since MSDI and NMSDI are based on information about precipitation and streamflow deficits, the detected drought frequencies are between those of SPI and SSFI. The drought duration and intensity identified by MSDI and NMSDI are found to be larger than those identified by SPI and SSFI because MSDI and NMSDI capture the drought onset in a way that is similar to SPI and capture drought termination and persistence in a way that is similar to SSFI.

In addition, the historical severe-drought records in the WRB were obtained to examine the performance of NMSDI. Our results show that the timing of the low NMSDI values match well with the drought occurrence indicated by the available records. Especially, two typical drought events that occurred in 2003 and 2008 (YRCC 2004, 2009) are identified well by the NMSDI (Fig. 2b). Given the comprehensiveness and effectiveness of NMSDI for drought characterization, it was adopted for our further investigations on the characteristics of historical drought evolution in the WRB.

b. The spatial pattern of NMSDI in the WRB

Figure 4 shows the averages of annual NMSDI in each subarea. Negative values indicate dry conditions, and vice versa for the positive values. The detailed classifications are shown in Table 2. Overall, all of the subareas have experienced a certain degree of drought, which exhibited a distinct spatial pattern at the subbasin level. In specific terms, the historical drought risks experienced in the middle basin including the Zhangjiashan (ZJSP), Lintong–Huaxian (LHP), Xianyang–Lintong (XLP), and Beidao–Linjiacun (BLP) partitions are lower than in other areas, as indicated by the smaller magnitude of negative NMSDI values. The highest risks of droughts occurring in the WRB are located in the subbasins of the Linjiacun–Weijiabu (LWP) and Zhuangtou (ZTP) partitions as shown by the largest magnitude of negative NMSDI values.

c. The temporal pattern of NMSDI

The MMK trend-test method was used to calculate the trend of monthly and annual NMSDI of each subarea in the WRB (Table 4). An increasing risk of droughts is found by the negative trends of monthly NMSDI in the
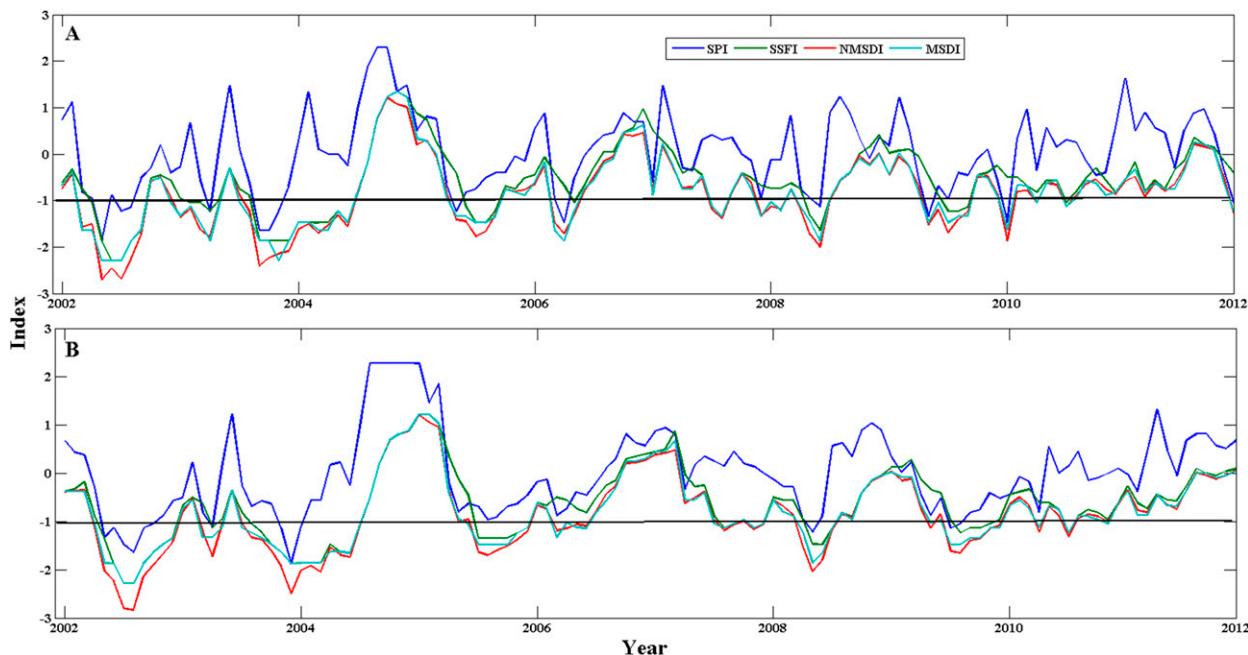
FIG. 3. Comparison for (a) 3- and (b) 6-month NMSDI, MSDI, SPI, and SSFI series covering 2002–11.

WRB, especially in March, April, May, July, and September. For the Beidao partition (BDP), the monthly NMSDI has decreased significantly for all months at the 95% confidence level and has experienced the most significant decreasing trend when compared with other subareas. Nonsignificant changes trends are found in January and February in the eastern part of the WRB (including XLP, LHP, and ZTP). On a annual time frame, a statistically significant downward tendency is detected for all subareas at the 99% confidence level. In general, our results show that the drought-prone region has experienced an increasing risk of droughts that posed great challenges for the sustainable development of local agriculture, the economy, and society.

d. The persistence of drought in the WRB

How will the historical droughts persist in the future? Figure 5 shows the values of Hurst index for the annual NMSDI of each subarea in the WRB. The values of Hurst index are larger than 0.5 in all subbasins except ZJSP, which has a value of Hurst index that is slightly smaller than 0.5. This result indicates that the decreasing trend of annual NMSDI may be persistent to a certain extent in most parts of the WRB. In other words, the historical droughts in the WRB will probably continue in the future. In contrast, the decreasing trend of annual NMSDI in ZJSP will become the opposite in the future, implying that the drought condition in this region may be mitigated to a certain degree. Our results have great implications for making effective adaptation strategies

to reduce possible damages caused by droughts at the subbasin level. Note, however, that drought persistence as analyzed here is by nature a projection of possible conditions in a probabilistic way. Physically based approaches such as driving a hydrological model with output from global or regional climate models should be adopted in the future.

e. The period of annual NMSDI in the WRB

In addition to the change trends, we examine the period of annual NMSDI, which can help to better understand historical droughts and facilitate drought predictions. Here, wavelet analysis on the basis of the Morlet wavelet (Huang et al. 2014b) is utilized, and the time-frequency distribution of annual NMSDI series is exhibited in Fig. 6. Red in Fig. 6 represents positive phase, and blue denotes negative phase; green and yellow are between positive and negative phases. The alternation between positive and negative phases is

TABLE 3. Statistics summarizing the frequency (events), mean duration (months), and intensity of droughts identified by SPI, SSI, MSDI, and NMSDI for the study period in the whole WRB. MSDI was developed by Hao and AghaKouchak (2013), and the calculation code was obtained online (http://amir.eng.uci.edu/software.php).

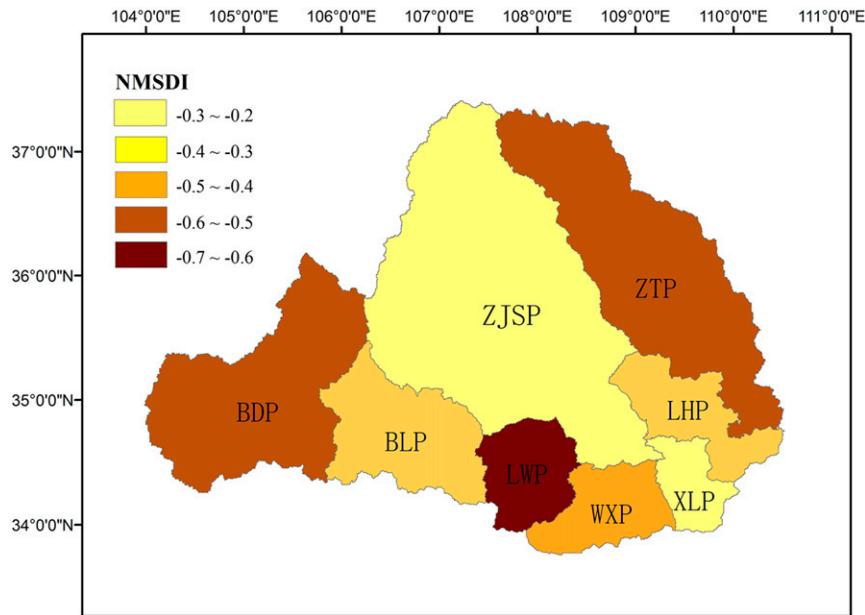| Statistics	SPI	SSI	MSDI	NMSDI
Frequency	95	47	73	69
Duration	1.35	3.11	3.26	3.43
Intensity	0.87	0.84	1.16	1.23

FIG. 4. The spatial distribution of mean annual 1-month NMSDI in each subarea in the WRB.

taken as the period of historical droughts. Results show that a primary period up to 20 years and a secondary period of ~7 years of annual NMSDI series exist, indicating interdecadal oscillations of droughts in the WRB. Dou and Yan (2013) studied the linkage of drought/flood in the Guanzhong Plain (located in the WRB) with sunspot activity and found a negative linkage in the 1960s and a positive relationship after the 1970s. Because the major objective is to develop a reliable integrated drought index and to characterize drought evolution, a further physical explanation for these periods should be explored in the future.

f. The identification of changepoints of annual NMSDI

The heuristic segmentation method was applied to identify the changepoints of annual NMSDI series in each subarea in the WRB. The threshold P_0 was selected as 0.95, and ℓ_0 was chosen as 25 following Bernaola-Galván et al. (2001). The results of detected changepoints in BDP and LHP are shown in Fig. 7. One changepoint was detected in BDP during its first iteration (Fig. 7a). For the second iteration, no changepoints were identified because the probability of the largest T was smaller than the threshold. Figure 7b indicates two changepoints in LHP during the two iterations because the probabilities of their largest T were larger than the threshold. Identified changepoints in other partitions are summarized in Table 5.

In general, the annual NMSDI series in the WRB is not stationary, with changepoints detected mainly in the early 1970s and mid-1990s (Table 5). It is worth mentioning that a large number of reservoirs and irrigation canals were constructed in the early 1970s—for

TABLE 4. The trends of monthly and annual NMSDI for each subarea in the WRB. WXP is the Weijiabu–Xianyang partition, and the remaining partitions are defined in the text (see Fig. 1). The * and ** represent significance at the 95% and 99% confidence levels, respectively.

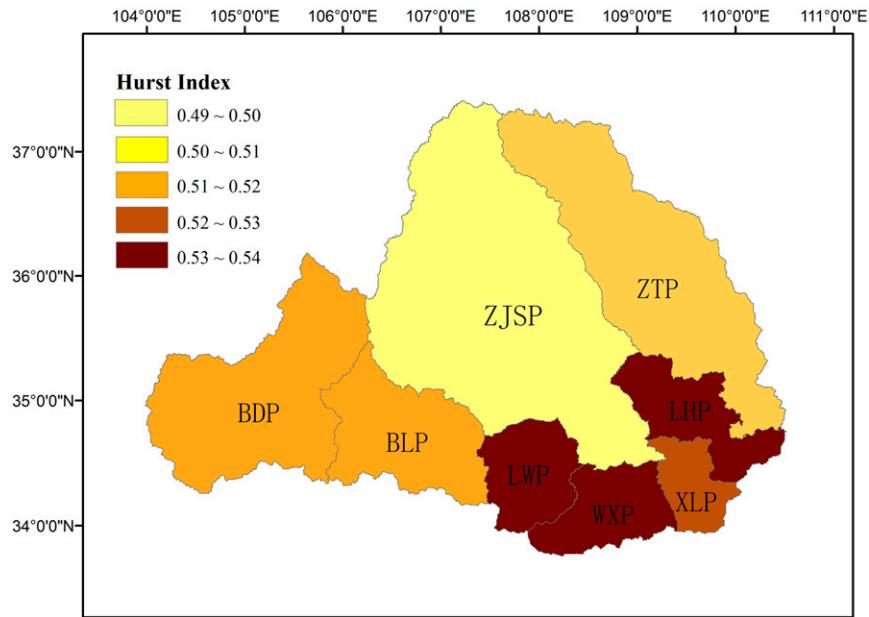| Subareas	Jan	Feb	Mar	Apr	May	Jun	Jul	Aug	Sep	Oct	Nov	Dec	Annual trend
BDP	−2.1*	−2.6**	−3.8**	−4.4**	−3.3**	−2.5*	−3.0**	−2.6**	−3.8**	−2.2*	−4.2**	−3.9**	−4.8**
BLP	0.4	−1.1	−2.9**	−5.0**	−3.3**	−2.2*	−2.9**	−2.0*	−3.1**	−2.2*	−3.9	−1.1	−4.2**
LWP	−2.4*	−1.7	−3.7**	−5.0**	−3.5**	−1.5	−2.8**	−1.0	−2.3*	−2.1*	−4.0	−1.6	−4.7**
WXP	−2.2*	−1.6	−2.7**	−4.2**	−3.6**	−1.0	−2.5*	−0.8	−2.3*	−2.2*	−3.3	−1.2	−3.8**
ZJSP	−0.5	0.1	−2.2*	−4.4**	−3.1**	−1.2	−2.0*	−1.3	−2.9**	−1.9*	−3.6	−1.2	−4.5**
XLP	0.3	0.1	−1.2	−3.5**	−2.3*	−0.2	−1.3	0.9	−2.0*	−1.6	−2.8	−0.1	−2.7**
LHP	0.6	0.1	−1.9	−4.0**	−2.7**	−0.4	−2.3*	−0.2	−2.2*	−1.6	−2.4	−0.2	−3.2**
ZTP	0.9	1.1	−1.9	−2.8**	−1.9	−0.9	−2.0*	−1.4	−2.4*	−1.3	−2.2	−0.4	−3.4**

FIG. 5. The spatial distribution of Hurst index in each subarea in the WRB.

example, the Yangmaowan and Fengcun reservoirs in 1970, the Baojixia canal in 1971, and the Dayu and Shimen reservoirs in 1972. These water projects were used for withdrawal of large amounts of water from the Wei River and have greatly changed the intra-annual characteristics of streamflow. In addition, soil conservation measures in the WRB were performed in the 1950s and have expanded on a large scale since the early 1970s. Soil conservation practices further alter local microtopography, rainfall interception, and infiltration rate, thereby reducing local streamflow and resulting in hydrological drought (Chang et al. 2014). Because precipitation has a nonsignificant decreasing trend in the WRB (Huang et al. 2015), construction of water projects and soil conservation practices may be the major driving forces resulting in the identified
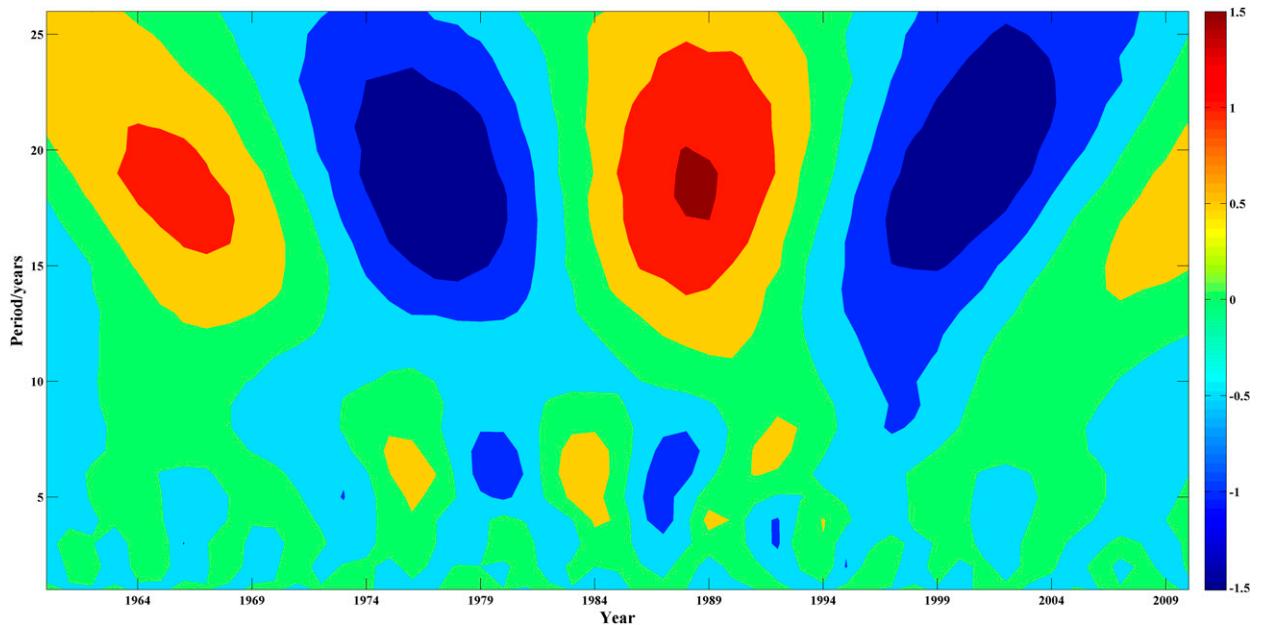

FIG. 6. The time-frequency distribution of annual 1-month NMSDI in the whole basin.
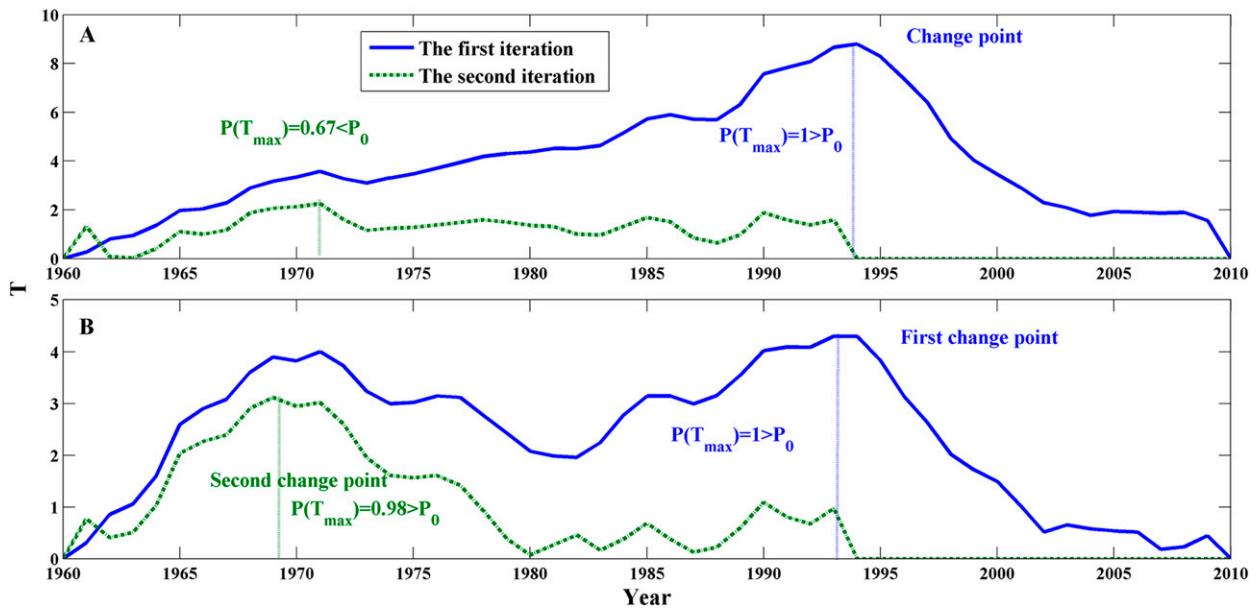
FIG. 7. The identification results of changepoints in (a) BDP and (b) LHP.

changepoints. The developed NMSDI in this study is based on coupled information for precipitation and streamflow. Hence, human activities in the WRB have lowered the drought index to a certain extent, mainly through affecting streamflow, although the quantitative effects require more investigations in the future.

5. Summary and conclusions

Drought index is the key for water-resource management and drought mitigation. A drought index that is based on a single variable is not sufficient for characterizing droughts comprehensively and effectively. By assuming that samples follow a particular probability density function, most parametric multivariate approaches would lead to large deviations of tails (e.g., the low or high quantiles). In this study, we build our efforts upon the work of Hao and AghaKouchak (2014) by proposing an additional nonparametric multivariate drought index using a kernel estimator. The newly proposed drought index was applied in the WRB in China, on the basis of which the change trends, persistence, periods, and changepoints are investigated. The four primary conclusions are as follows:

1) In general, NMSDI captures the drought onset in a way that is similar to that of SPI and captures drought termination and persistence in ways that are similar to the performance of SSFI. Consistence is also found when comparing NMSDI with an existing multivariate standardized drought index at 1-, 3-, and 6-month time scales. Through comprehensive validations against

existing drought indices and collected historical drought records, our results demonstrate that NMSDI is an effective tool for drought characterization.

2) NMSDI in the WRB shows a noticeable spatial gradient, with larger drought risk experienced in the LWP than in other areas. The drought-prone region has experienced an increasing trend of droughts in most of the subbasins at monthly and annual scales—a trend that may persist, to a certain extent, in the future.

3) A primary period of ~20 years and a secondary period of ~7 years of annual NMSDI series in the WRB were found.

4) The identified changepoints of annual NMSDI are mainly concentrated in the early 1970s and mid-1990s and may be caused by the construction of water projects and by soil conservation practices in the WRB.

Similar to existing multivariable drought indices, advantages and disadvantages do exist. The advantages of the NMSDI that was developed in this study are that the

TABLE 5. The detected changepoints in each subarea in the WRB.

Subareas	Changepoint(s)
BDP	1994
BLP	1994
LWP	1969, 1994
WXP	1971, 1994
ZJSP	1994
XLP	1971, 1994
LHP	1969, 1993
ZTP	1994

index is distribution free and has exhibited good performance when compared with the corresponding SPI and SSFI (the correlation coefficients are 0.83 and 0.81, respectively) and with the available historical drought records. In general, the variations of NMSDI can be used to capture drought onset in a way that is similar to SPI and can capture drought termination and persistence in ways similar to those of SSFI; that is, it is more sensitive to capturing the onset, persistence, and termination of droughts, thereby integrating the useful information found in SPI and SSFI. When comparing NMSDI with the existing MSDI, high consistence is found for the temporal variations of the two drought indices at various time scales, confirming the validity of the newly constructed NMSDI in drought detections. NMSDI is more sensitive in capturing drought onset and termination than MSDI is at the 1-month time scale, demonstrating the added value of the newly developed nonparametric drought index in capturing drought characteristics. Note, however, that this paper does not claim that NMSDI alone is always sufficient for capturing drought characteristics. In fact, previous studies have highlighted the limitations of various drought indicators. Having an additional source of information can provide additional insights in drought-index development and can improve our understanding of drought development. Identifying whether and where the new drought index would be particularly advantageous will require more in-depth research over a larger research domain with varying hydroclimatic regimes. Moreover, the NMSDI developed in this study is only coupled with the deficits of precipitation and streamflow because of the limitation of the nonparametric kernel estimator. More efforts are still needed in the future toward developing a drought index that can couple meteorological, hydrological, and agricultural factors in an efficient way.

REFERENCES

AghaKouchak, A., 2015: A multivariate approach for persistence-based drought prediction: Application to the 2010–2011 East Africa drought. *J. Hydrol.*, **526**, 127–135, doi:10.1016/j.jhydrol.2014.09.063.

——, and N. Nakhjiri, 2012: A near real-time satellite-based global drought climate data record. *Environ. Res. Lett.*, **7**, 044037, doi:10.1088/1748-9326/7/4/044037.

Bernaola-Galván, P., P. C. Ivanov, L. A. Nunes Amaral, and H. E. Stanley, 2001: Scale invariance in the nonstationarity of human heart rate. *Phys. Rev. Lett.*, **87**, 160815, doi:10.1103/PhysRevLett.87.168105.

Chang, J. X., Y. Wang, and E. Istanbulluoglu, 2014: Impact of climate change and human activities on runoff in the Weihe River basin, China. *Quat. Int.*, **380–381**, 169–179, doi:10.1016/j.quaint.2014.03.048.

Dai, A., 2011: Characteristics and trends in various forms of the Palmer drought severity index during 1900–2008. *J. Geophys. Res.*, **116**, D12115, doi:10.1029/2010JD015541.

Dou, L., and A. Yan, 2013: Relationships between drought and flood disasters in Guanzhong plain and the activities of sunspot (in Chinese). *J. Arid Land Resour. Environ*, **27**, 76–82. [Available online at http://d.wanfangdata.com.cn/Periodical/ghqzyyhj201308013.]

Farahmand, A., and A. AghaKouchak, 2015: A generalized framework for deriving nonparametric standardized drought indicators. *Adv. Water Resour.*, **76**, 140–145, doi:10.1016/j.advwatres.2014.11.012.

Feng, G.-L., Z.-Q. Gong, W.-J. Dong, and J.-P. Li, 2005: Abrupt climate change detection based on heuristic segmentation algorithm (in Chinese). *Wuli Xuebao*, **54**, 5494–5499. [Available online at http://wulixb.iphy.ac.cn/EN/abstract/abstract10262.shtml.]

Hamed, K. H., and A. R. Rao, 1998: A modified Mann–Kendall trend test for autocorrelated data. *J. Hydrol.*, **204**, 182–196, doi:10.1016/S0022-1694(97)00125-X.

Hao, Z., and A. AghaKouchak, 2013: Multivariate standardized drought index: A multi-index parametric approach for drought analysis. *Adv. Water Resour.*, **57**, 12–18, doi:10.1016/j.advwatres.2013.03.009.

——, and ——, 2014: A nonparametric multivariate multi-index drought monitoring framework. *J. Hydrometeor.*, **15**, 89–101, doi:10.1175/JHM-D-12-0160.1.

——, and V. P. Singh, 2015: Drought characterization from a multivariate perspective: A review. *J. Hydrol.*, **527**, 668–678, doi:10.1016/j.jhydrol.2015.05.031.

Heim, R. R., 2002: A review of twentieth-century drought indices used in the United States. *Bull. Amer. Meteor. Soc.*, **83**, 1149–1166, doi:10.1175/1520-0477(2002)083<1149:AROTDI>2.3.CO;2.

Hosking, J. R. M., 1984: Modeling persistence in hydrological time series using fractional differencing. *Water Resour. Res.*, **20**, 1898–1908, doi:10.1029/WR020i012p01898.

Huang, S., J. Chang, Q. Huang, and Y. Chen, 2014a: Spatio-temporal changes and frequency analysis of drought in the Wei River basin, China. *Water Resour. Manage.*, **28**, 3095–3110, doi:10.1007/s11269-014-0657-4.

——, B. Hou, J. Chang, Q. Huang, and Y. Chen, 2014b: Copulas-based probabilistic characterization of the combination of dry and wet conditions in the Guanzhong Plain, China. *J. Hydrol.*, **519**, 3204–3213, doi:10.1016/j.jhydrol.2014.10.039.

——, J. Chang, Q. Huang, and Y. Chen, 2015: Identification of abrupt changes of the relationship between rainfall and runoff in the Wei River basin, China. *Theor. Appl. Climatol.*, **120**, 299–310, doi:10.1007/s00704-014-1170-7.

Hurst, H. E., 1956: Method of using long-term storage in reservoirs. *Proc. Inst. Civ. Eng.*, **5**, 519–543, doi:10.1680/iicep.1956.11503.

Kao, S. C., and R. S. Govindaraju, 2010: A copula-based joint deficit index for droughts. *J. Hydrol.*, **380**, 121–134, doi:10.1016/j.jhydrol.2009.10.029.

Kendall, M. G., 1955: *Rank Correlation Methods.* Griffin, 272 pp.

Keyantash, J. A., and J. A. Dracup, 2004: An aggregate drought index: Assessing drought severity based on fluctuations in the hydrologic cycle and surface water storage. *Water Resour. Res.*, **40**, W09304, doi:10.1029/2003WR002610.

Kim, T. W., J. B. Valdés, and C. Yoo, 2003: Nonparametric approach for estimating return periods of droughts in arid regions. *J. Hydrol. Eng.*, **8**, 237–246, doi:10.1061/(ASCE)1084-0699(2003)8:5(237).

Lall, U., 1995: Recent advances in nonparametric function estimation: Hydrologic applications. *Rev. Geophys.*, **33**, 1093–1102, doi:10.1029/95RG00343.

——, B. Rajagopalan, and D. G. Tarboton, 1996: A nonparametric wet/dry spell model for resampling daily precipitation. *Water Resour. Res.*, **32**, 2803–2823, doi:10.1029/96WR00565.

Leng, G., Q. Tang, and S. Rayburg, 2015: Climate change impacts on meteorological, agricultural and hydrological droughts in China. *Global Planet. Change*, **126**, 23–34, doi:10.1016/j.gloplacha.2015.01.003.

——, ——, S. Huang, X. Zhang, and J. Cao, 2016: Assessments of joint hydrological extreme risks in a warming climate in China. *Int. J. Climatol.*, **36**, 1632–1642, doi:10.1002/joc.4447.

Mann, H. B., 1945: Nonparametric tests against trend. *Econometrica*, **13**, 245–259, doi:10.2307/1907187.

McKee, T. B., N. J. Doesken, and J. Kleist, 1993: The relationship of drought frequency and duration to time scales. Preprints, *Eighth Conf. on Applied Climatology*, Anaheim, CA, Amer. Meteor. Soc., 179–184.

Mishra, A. K., and V. P. Singh, 2010: A review of drought concepts. *J. Hydrol.*, **391**, 202–216, doi:10.1016/j.jhydrol.2010.07.012.

——, and ——, 2011: Drought modeling—A review. *J. Hydrol.*, **403**, 157–175, doi:10.1016/j.jhydrol.2011.03.049.

Moon, Y., and U. Lall, 1994: Kernel quantile function estimator for flood frequency analysis. *Water Resour. Res.*, **30**, 3095–3103, doi:10.1029/94WR01217.

Oliver, R., and J. L. Ballester, 1996: Rescaled range analysis of the asymmetry of solar activity. *Sol. Phys.*, **169**, 215–224, doi:10.1007/BF00153842.

Palmer, W. C., 1968: Keeping track of crop moisture conditions, nationwide: The new crop moisture index. *Weatherwise*, **21** (4), 156–161, doi:10.1080/00431672.1968.9932814.

Pandey, R. P., and K. S. Ramasastri, 2001: Relationship between the common climatic parameters and average drought frequency. *Hydrol. Processes*, **15**, 1019–1032, doi:10.1002/hyp.187.

Quiring, S., J. W. Nielsen-Gammon, R. Srinivasan, T. Miller, and B. Narasimhan, 2007: Drought monitoring index for Texas. Texas Water Development Board Final Tech. Rep., 262 pp. [Available online at http://www.twdb.texas.gov/publications/reports/contracted_reports/doc/2005483028_drought_index.pdf.]

Sadri, S., and D. H. Burn, 2012: Nonparametric methods for drought severity estimation at ungauged sites. *Water Resour. Res.*, **48**, W12505, doi:10.1029/2011WR011323.

Scott, D. W., 1992: *Multivariate Density Estimation: Theory, Practice and Visualization.* Wiley Series in Probability and Statistics, John Wiley and Sons, 336 pp.

Sepulcre-Canto, G., S. Horion, A. Singleton, H. Carrao, and J. Vogt, 2012: Development of a combined drought indicator to detect agricultural drought in Europe. *Nat. Hazards Earth Syst. Sci.*, **12**, 3519–3531, doi:10.5194/nhess-12-3519-2012.

Sharma, A., 2000: Seasonal to interannual rainfall probabilistic forecasts for improved water supply management: Part 3—A nonparametric probabilistic forecast model. *J. Hydrol.*, **239**, 249–258, doi:10.1016/S0022-1694(00)00348-6.

Sheffield, J., E. F. Wood, and M. L. Roderick, 2012: Little change in global drought over the past 60 years. *Nature*, **491**, 435–438, doi:10.1038/nature11575.

——, and Coauthors, 2014: A drought monitoring and forecasting system for sub-Sahara African water resources and food security. *Bull. Amer. Meteor. Soc.*, **95**, 861–882, doi:10.1175/BAMS-D-12-00124.1.

Sherwood, S., and Q. Fu, 2014: A drier future? *Science*, **343**, 737–739, doi:10.1126/science.1247620.

Shukla, S., and A. W. Wood, 2008: Use of a standardized runoff index for characterizing hydrologic drought. *Geophys. Res. Lett.*, **35**, L02405, doi:10.1029/2007GL032487.

——, A. C. Steinemann, and D. P. Lettenmaier, 2011: Drought monitoring for Washington State: Indicators and applications. *J. Hydrometeor.*, **12**, 66–83, doi:10.1175/2010JHM1307.1.

Silverman, B. W., 1986: *Density Estimation for Statistics and Data Analysis.* Chapman and Hall, 176 pp.

Smakhtin, V. U., 2001: Low flow hydrology: A review. *J. Hydrol.*, **240**, 147–186, doi:10.1016/S0022-1694(00)00340-1.

Spinoni, J., G. Naumann, H. Carrao, P. Barbosa, and J. V. Vogt, 2014: World drought frequency, duration, and severity for 1951–2010. *Int. J. Climatol.*, **34**, 2792–2804, doi:10.1002/joc.3875.

Telesca, L., M. Lovallo, L. Lopez-Moreno, and S. Vicente-Serrano, 2012: Investigation of scaling properties in monthly streamflow and standardized streamflow index (SSI) time series in the Ebro basin (Spain). *Physica A*, **391**, 1662–1678, doi:10.1016/j.physa.2011.10.023.

Torrence, C., and G. P. Compo, 1998: A practical guide to wavelet analysis. *Bull. Amer. Meteor. Soc.*, **79**, 61–78, doi:10.1175/1520-0477(1998)079<0061:APGTWA>2.0.CO;2.

Trenberth, K. E., A. Dai, G. van der Schrier, P. D. Jones, J. Barichivich, K. R. Briffa, and J. Sheffield, 2014: Global warming and changes in drought. *Nat. Climate Change*, **4**, 17–22, doi:10.1038/nclimate2067.

van der Schrier, G., J. Barichivich, K. R. Briffa, and P. D. Jones, 2013: A scPDSI-based global dataset of dry and wet spells for 1901–2009. *J. Geophys. Res. Atmos.*, **118**, 4025–4048, doi:10.1002/jgrd.50355.

Vicente-Serrano, S. M., S. Beguería, and J. I. López-Moreno, 2010: A multiscalar drought index sensitive to global warming: The standardized precipitation evapotranspiration index. *J. Climate*, **23**, 1696–1718, doi:10.1175/2009JCLI2909.1.

Wang, C. S. H., L. Bauwens, and C. Hsiao, 2013: Forecasting a long memory process subject to structural breaks. *J. Econom.*, **177**, 171–184, doi:10.1016/j.jeconom.2013.04.006.

Wells, N., S. Goddard, and M. J. Hayes, 2004: A self-calibrating Palmer drought severity index. *J. Climate*, **17**, 2335–2351, doi:10.1175/1520-0442(2004)017<2335:ASPDSI>2.0.CO;2.

Wilhite, D. A., 2000: Drought as a natural hazard: Concepts and definitions. *Drought: A Global Assessment*, D. A. Wilhite, Ed., Hazards Disasters Series, Vol. I, Routledge, 3–18.

——, 2005: *Drought and Water Crises: Science, Technology, and Management Issues.* Taylor and Francis, 406 pp.

Winslow, M. D., J. V. Vogt, R. J. Thomas, S. Sommer, C. Martius, and M. Akhtar-Schuster, 2011: Science for improving the monitoring and assessment of dryland degradation. *Land Degrad. Dev.*, **22**, 145–149, doi:10.1002/ldr.1044.

WMO, 2006: Drought monitoring and early warning: Concepts, progress and future challenges. World Meteorological Organization Doc. WMO-No. 1006, 26 pp. [Available online at http://www.droughtmanagement.info/literature/WMO_drought_monitoring_early_warning_2006.pdf.]

YRCC, 2004: Yellow River Water Resources Bulletin (in Chinese). Yellow River Conservancy Commission Annual Rep. [Available online at http://www.yellowriver.gov.cn/other/hhgb/2004.htm.]

——, 2009: Yellow River Water Resources Bulletin (in Chinese). Yellow River Conservancy Commission Annual Rep., 40 pp. [Available online at http://www.yellowriver.gov.cn/other/hhgb/2009/2009.html.]

Zhang, H., Y. Chen, and G. Ren, 2008: The characteristics of precipitation variation of Weihe River basin in Shaanxi Province during recent 50 years (in Chinese). *Agric. Res. Arid Areas*, **26**, 236–242.